Endophytic pyrroloquinoline quinone enhances banana growth and immunity against *Fusarium* wilt for plant-microbe mutualisms

Running Title: PQQ coordinates plant growth and immunity

Shih-Hsun Walter Hung[1,2,3,4], Man-Yun Yu[1], Chia-Ho Liu[1], Tsai-Ching Huang[1], Jian-Hau Peng[5,6], Nai-Yun Jang[1], Chih-Horng Kuo[2,5,6,7], Yu-Liang Yang[8], Ying-Ning Ho[9,10,11], En-Pei Isabel Chiang[3,4,5,6,12], Hau-Hsuan Hwang[1,3,4,5,6], and Chieh-Chen Huang[1,3,4,5,6]*

[1] Department of Life Sciences, National Chung Hsing University, Taichung 402202, Taiwan

[2] Institute of Plant and Microbial Biology, Academia Sinica, Taipei 115201, Taiwan

[3] Advanced Plant and Food Crop Biotechnology Center, National Chung Hsing University, Taichung 402202, Taiwan

[4] Innovation and Development Centre of Sustainable Agriculture, National Chung Hsing University, Taichung 402202, Taiwan

[5] PhD Program in Microbial Genomics, National Chung Hsing University, Taichung 402202, Taiwan

[6] PhD Program in Microbial Genomics, Academia Sinica, Taipei 115201, Taiwan

[7] Biotechnology Center, National Chung Hsing University, Taichung 402202, Taiwan

[8] Agricultural Biotechnology Research Center, Academia Sinica, Taipei, 115201 Taiwan

[9] Institute of Marine Biology, College of Life Science, National Taiwan Ocean University, Keelung 202301, Taiwan

[10] Center of Excellence for the Oceans, National Taiwan Ocean University, Keelung 202301, Taiwan

[11] Taiwan Ocean Genome Center, National Taiwan Ocean University, Keelung 202301, Taiwan

[12] Department of Food Science and Biotechnology, National Chung Hsing University, Taichung 402202, Taiwan

***Correspondence**: Chieh-Chen Huang; cchuang@dragon.nchu.edu.tw

ORCID SHW Hung, 0000-0002-8749-5653; CH Liu, 0000-0001-9166-3966; TC Huang, 0000-0002-3410-2051; JH Peng, 0000-0001-6052-8606; CH Kuo, 0000-0002-2857-0529; YL Yang, 0000-0002-3533-5148; YN Ho, 0000-0003-0943-1416; EPI Chiang, 0000-0002-0158-0962; HH Hwang, 0000-0001-9132-0242; CC Huang, 0000-0002-3739-6315.

Keywords: endophyte, symbiosis, pyrroloquinoline quinone (PQQ), *Fusarium* wilt of banana, molecular plant-microbe interactions (MPMI)

Abstract

Fusarium wilt has a substantial impact on global banana production, posing a threat to food security worldwide. However, breeding new *Fusarium*-resistant cultivars is difficult and time-consuming. Alternatively, endophytic biostimulants that could combat such pervasive plant diseases provide possible novel solutions. Our prior research demonstrated that a pyrroloquinoline quinone (PQQ)–producing endophytic bacterium, *Burkholderia seminalis* 869T2, can enhance the growth of various plant species and protect bananas from *Fusarium* wilt in the field. PQQ is a peptide-derived redox cofactor known to stimulate mitochondrial biogenesis and metabolism in animals, but its molecular roles, especially in plants, remain to be elucidated. In this study, multi-omics approaches were employed to explore the potential mechanisms through which PQQ influences banana plants. The result of *in situ* imaging mass spectrometry revealed that the endophytic metabolite PQQ does not function through direct antagonism against *Fusarium*. The follow-up transcriptomic profiling shows it could regulate plant respiration, TCA cycle, oxidative phosphorylation, NAD/NADP–dependent dehydrogenases, MAPK signalling, and various phytohormone signalling pathways. Furthermore, PQQ appeared to trigger plant systemic immunity, thereby enhancing plant health and resistance to biotic stress. Beyond that, the complete genome of 869T2 was determined for follow-up comparative genomics analyses, revealing its genetic contexts, potential evolutionary events of PQQ operons among the *Burkholderia* species, and the absence of human virulence-facilitating genes within those PQQ-producing agricultural isolates. In summary, this study facilitates our understanding of PQQ in plant-microbe mutualisms and provides scientific evidence for its future application in agriculture.

Significance Statement

Fusarium wilt is caused by *Fusarium oxysporum* f. sp. *cubense* tropical race 4 (*Foc* TR4), a notorious soil-borne pathogen that attacks bananas' vascular system, which critically threatens global banana production and food security. A potential PQQ-producing endophytic strain has been confirmed to protect bananas through *in planta* biocontrol, reducing the morbidity of Banana *Fusarium* Wilt (BFW) disease in the field and promoting the growth of banana plants simultaneously. Our results revealed that the endophytic metabolite PQQ does not function through direct antagonism but triggers plant systemic immunity and coordinates energetic metabolisms, thereby improving the overall health of host plants and enhancing their resistance against *Fusarium* wilt.

66 **Main Text**

67 ## Introduction

68 Pyrroloquinoline quinone (PQQ), also known as methoxatin, was initially identified as
69 a unique quinone-like cofactor that partners with bacterial glucose and alcohol
70 dehydrogenases, as reported in early studies (1, 2). Subsequent research uncovered a
71 variety of PQQ-dependent dehydrogenases in prokaryotes, which process substances like
72 methanol, alcohol, aldehydes, and sugars (3–5). Initially thought to be exclusive to
73 prokaryotes, PQQ was later discovered in eukaryotic organisms, including animals and
74 plants (6). Serving as a redox cofactor for several dehydrogenases, PQQ is integral to vital
75 metabolic processes across different life forms of kingdoms (7, 8). Its diverse benefits, both
76 in vivo and in vitro, have been demonstrated in numerous studies focusing on microbes and
77 animals. For example, PQQ acts as a powerful antioxidant by neutralizing reactive oxygen
78 species (ROS) (9), it helps maintain the balance of nicotinamide adenine dinucleotide levels
79 (9), and it stimulates the creation of mitochondria (10, 11), thereby enhancing energy-
80 related metabolisms such as oxidative phosphorylation and ATP production (12, 13).
81 However, the impact of PQQ on plant molecular biology is not well understood. Recent
82 findings suggest that PQQ can eliminate ROS in plants similarly to its function in animals
83 (14). Additionally, PQQ appears to enhance the glucose dehydrogenase activity and
84 phosphate-solubilizing abilities of plant growth-promoting bacteria (15–19), and it may also
85 bolster the antifungal defence of plants by supporting plant-associated microbes (20, 21).
86 Nevertheless, the precise molecular mechanisms underlying these effects are still to be
87 elucidated.

88 On the other hand, *Fusarium oxysporum* f. sp. *cubense* tropical race 4 (*Foc* TR4) is a
89 notorious soil-borne pathogen that attacks the vascular system of bananas, critically
90 threatening banana production and having severe consequences on global food security
91 and the livelihoods of around 400 million people (22, 23). The most effective approach to
92 combat this highly destructive and aggressive fungus is to prevent its initial spread, as it can
93 cause complete yield loss once established in a field (24). Currently, over 80% of global
94 banana production relies on Foc TR4-susceptible germplasm (25). Given the challenge of
95 breeding new varieties or cultivars that are both suitable for the value chain and resistant to
96 disease, new technologies for accelerating precise breeding and biological agents for in-
97 field protection are urgently needed. Some plant symbionts have been reported to protect
98 banana plants against *Foc* TR4 (26–29), and some microbial metabolites function as
99 biostimulants, resulting in plant disease protection through exogenous supplementation (30,
100 31).

101 Our previous works isolated and characterised a potential PQQ-producing
102 endophyte, *Burkholderia seminalis* 869T2, which confers strong resistance to *Fusarium*
103 *oxysporum* f. sp. *cubense* tropical race 4 (Foc TR4) (28, 32). This endophytic strain has
104 been confirmed to protect bananas in field tests through *in planta* biocontrol, reducing the

105 morbidity of Banana *Fusarium* Wilt disease from 24.5% to 3.4% while also promoting the
106 growth of banana plants (28). Besides those positive effects brought on bananas, strain
107 869T2 and its metabolites have been established as plant-beneficial or stress-resilient
108 endophytic biostimulants that promote the growth of various crops, including *Brassica*,
109 *Lactuca*, *Amaranthus*, *Capsicum*, and *Abelmoschus* (33, 34). The strain has also been
110 established as a versatile endophytic biostimulant for leafy vegetables. It significantly
111 promotes plant growth and enhances crop quality by increasing harvested head weight, size
112 and nutrient composition. Additionally, a two-week acceleration in harvest time and 50%
113 savings on fertilising costs result in reducing costs and increasing product value
114 simultaneously, which provides a model for in-field endophytic biostimulants-assisted smart
115 agricultural management for lettuce production (34). On the other hand, the bioremediation
116 availability of 869T2 for the degradation of persistent organic pollutants (POPs), such as
117 dioxins, under an aerobic environment through 2-haloacid dehalogenase has also been
118 demonstrated (35). These results emphasize the importance of endophytic bacteria,
119 warranting further investigation due to their enigmatic symbiotic relationships with hosts and
120 potential applications in the agro-industry.

121 In this study, our goal was to better understand the molecular mechanisms of
122 endophytic PQQ *in planta*, particularly in the context of plant-microbe mutualistic symbiosis
123 and the defence against pathogens. Our result revealed that endophytic PQQ has no direct
124 antagonism activity to inhibit the growth of *Fusarium* species. Instead, it promotes the
125 overall health of host plants by triggering plant immunity through the modulation of multiple
126 phytohormones and MAPK signalling pathways. Additionally, it coordinates their energetic
127 metabolisms, including the TCA cycle, oxidative phosphorylation, and the biosynthesis and
128 activity of NAD/NADP-dependent enzymes. Meanwhile, the results of comparative
129 genomics shed light on the evolution of the pqq operon and other genetic contents, thus
130 offering clues about the co-evolution and mutualistic relationships among those plant-
131 associated bacteria with their hosts.

132 ## Results

133 ### Species reclassification of strain 869T2 to *Burkholderia seminalis*

134 Strain 869T2 was initially identified as *Burkholderia cenocepacia* with its draft
135 genome sequence (32). However, updated analysis of molecular phylogeny and gene
136 content indicated that this strain is more similar to *B. seminalis* (36). Therefore, complete
137 genome sequencing and comparative analyses were performed in this work to determine its
138 species assignment.

139 For hybrid *de novo* assembly, 2 x 3,178,899 (~1.9 Gb) of Illumina and 46,153 (~0.5
140 Gb) of untrimmed ONT raw reads were generated, which provided ~238- and ~65-fold
141 coverages for this genome, respectively. The assembly result indicated that 869T2 has
142 three circular chromosomes totalling 8,022,336 bp and an average GC content of 67.03%.
143 The comparison against a reference Burkholderiales dataset identified 687 complete
144 BUSCOs (99.9%), one fragmented BUSCOs (0.1%), and no missing BUSCOs within this
145 genome assembly, supporting that the genome assembly is complete. The annotation
146 showed that this genome contains six complete sets of rRNA genes, 67 tRNA genes, four
147 ncRNAs, 7,090 protein-coding genes and 112 pseudogenes (Table S1).

148 For the species assignment, the newly generated complete genome sequence was
149 utilised for comparative analysis with key representatives of *B. seminalis* and *B.*
150 *cenocepacia* (Table S2) based on genome-wide average nucleotide identity (ANI) and core-
151 genome phylogeny. The result showed that 869T2 shares ~93-95% of its genome with other
152 *B. seminalis* strains and has > 99% ANI (Fig. 1A). In contrast, 869T2 shares only ~79-82%
153 of its genome and has < 93% ANI when compared to *B. cenocepacia* strains. Additionally,
154 3,018 single-copy genes shared by all strains were identified and used to produce a
155 concatenated alignment containing 987,390 aligned amino acid sites for maximum
156 likelihood phylogeny inference (Fig. 1A). Based on 1,000 resamplings, the resulting tree had
157 100% bootstrap support value for all internal branches and 869T2 is a member of the *B.*
158 *seminalis* clade. Based on these results, strain 869T2 can be confidently re-classified as a
159 member of *B. seminalis*.

160

161 ### Gene content analysis between *B. cenocepacia* and *B. seminalis*

162 For more in-depth analysis, the gene content of representative *B. seminalis* and *B.*
163 *cenocepacia* strains was compared. Specifically, genes known to be related to
164 environmental adaptation and molecular plant-microbe interactions (MPMI) were the main
165 targets (Fig. 1B and Table S3). A distinct differentiation was observed for genes encode for
166 nitrile hydratase cluster (*nthAB*), phenylacetaldoxime dehydratase (*oxd*), galacturonate
167 metabolism (*uxa*), indoleacetic acid (IAA) biosynthesis (*iaaHM*), and pyrrolnitrin biosynthesis
168 (*prnABCD*); these genes were conserved among *B. seminalis* strains but mostly absent

169 among *B. cenocepacia* strains (Fig. 1B). Additionally, *B. seminalis* strains mostly have two
170 copies of genes for feruloyl esterase (*faeB*) and ACC deaminase (*acdS*). On the other hand,
171 genes involved in virulence to human (*esmR*, *amiI*, *cciI*, *cciR*, and *opcI*) (37) were found
172 only in *B. cenocepacia* strains, but absent in all of the *B. seminalis* strains examined (Fig.
173 1B), which mitigate the risk of using *B. seminalis* strains such as 869T2 for agricultural
174 application. Finally, the *pqq* operon, encoding essential genes responsible for the
175 biosynthesis of PQQ, is conserved in most of the strains examined.

176

177 **PQQ cannot antagonise *Fusarium in vitro***

178 Given that 869T2 has various plant-growth-promoting (PGP) traits and abundant
179 MPMI-related genetic contents, we used the ultra-high performance liquid chromatography-
180 tandem mass spectrometry (UHPLC-MS/MS) technique to determine its metabolome and
181 target the specific chemicals responsible for the PGP or pathogen resistance potential. The
182 results showed that 869T2 produces multiple phytohormones, including auxin, cytokinin,
183 gibberellic acid, ethylene and salicylic acid, as well as the corresponding regulatory factors
184 were confirmed (Table S4). Besides, 31 cyclic dipeptides (CDPs) were identified; some
185 CDPs were found as antimicrobial substances and antibiotics (Table S5). Furthermore,
186 along with a biosynthesis operon of pyrrolnitrin, an antibiotic that suppresses *Fusarium*
187 species (38), four of its antifungal derivates: iso-, oxy- and fluoro-pyrrolnitrin and 3-chloro-4-
188 (2-nitrophenyl)-1H-pyrrole were also detected. These results suggested that 869T2 could
189 inhibit the growth of fungi, *e.g.*, *Foc* TR4, via specific antifungal compounds.

190 A follow-up *in situ* metabolic investigation using the matrix-assisted laser desorption
191 ionization-time of flight (MALDI-TOF) imaging mass spectrometry (IMS) technique also
192 confirmed that 869T2 produced pyrrolnitrin and its derivatives, oxypyrrolnitrin or 3-Chloro-4-
193 (3-chloro-4-fluoro-2-nitrophenyl) pyrrole, to inhibit the growth *Foc* TR4 *in vitro* (Fig. 2A).
194 Strikingly, the signal of endophytic biostimulants PQQ was found and was only detected
195 when incubating without *Foc* TR4 (Fig. 2B); the endophytic PQQ production was further
196 confirmed through gas chromatography-mass spectrometry (GC-MS) by comparing to the
197 synthetic PQQ standard (>98% purity) (Fig. S1). Previous studies suggested mutagenesis
198 on *pqqC* and *pqqE*, essential genes for PQQ biosynthesis, affects the bacterial antimicrobial
199 activity *in vitro* or *in planta* (20, 21, 39). However, our imaging mass results suggested that
200 the production of PQQ seems irrelevant to the *Fusarium* inhibition. To explain this
201 paradoxical relationship, an antagonism assay was performed using levels of synthetic PQQ
202 standards as treatments and *B. seminalis* 869T2 as a control. The results showed that PQQ
203 has no positive effects on inhibiting the growth of *Foc* TR4 but improves it instead (Fig. 2C).
204 Based on this evidence, we raise another possibility that PQQ may induce plant immunity,
205 resulting in antimicrobial activity in plants. To examine our hypothesis, synthetic PQQ was
206 exogenously supplemented to banana plantlets, and the morbidity to *Fusarium* wilt and

207 plant transcriptomics were investigated to unveil the obscure molecular mechanisms among
208 them.

209

210 **Exogenous supplementation of PQQ induces the growth and development of banana**
211 **plants**

212 Firstly, 5 nM, 50 nM, 100 nM and 1000 nM PQQ, hereinafter referred to as P05, P50,
213 P100 and P1000, respectively, were examined on tissue culture banana plantlets; about
214 twenty biological replications were set for each treatment. At 48 days after treatment (DPT),
215 the results showed that exogenous PQQ supplementation contributes to the differentiation
216 of both shoot and root (Fig. 3A-C). Among them, by estimating using the developmental
217 indicator N_{50}, defined as the shoot/root length of the shortest organ at 50% of the total
218 shoot/root length, P100 seems an ideal dosage for triggering plant leaf and root
219 development. For root development: (a) P100 had three plantlets without visible root
220 development (CK had seven); (b) the root N_{50} of P100 was at level 7-8 (CK was at level 3-
221 4); (c) the maximum root order of P100 was at level >9 (CK was at level 5-6) (Fig. 3B). For
222 leaf development: (a) P100 had four plantlets without visible leaf development (CK had the
223 same); (b) the leaf N_{50} of P100 was at level 3 (CK was at level 2); (c) the maximum leaf
224 order of P100 was at level 5 (CK was at level 3) (Fig. 3C).

225 Besides, significantly more root and leaf numbers were both observed in P50 and
226 P100 (Fig. 3D,E); all treatments significantly elongated the root length (Fig. 3F) while only
227 P100 promoted the plant height compared to the CK with statistical significance (Fig. 3G).
228 These positive effects on plant growth and development were found to remain after the
229 bananas were transplanted to soil pots at least until 137 DPT (Fig. S2). Given that P1000
230 did not constantly improve plant growth and even contributed less than P100, we
231 hypothesise that a high dosage of PQQ supplementation may inhibit plant growth.
232 Therefore, additional experimental batches, including P100, P1000, and P2000 (2000 nM
233 PQQ), were performed to delineate the boundary of its working concentration. The
234 phenotypic results together suggested that the supplementation concentration over 100 nM
235 had no significant positive effects and, in some cases, harmed the plants instead (Fig. S3).
236 For instance, the fresh weight and plant height of the 1000 nM treatments decreased from
237 0.66 ± 0.06 g to 0.59 ± 0.08 g (Fig. S3B) and from 2.46 ± 0.13 cm to 2.25 ± 0.12 cm (Fig.
238 S3E), respectively. Accordingly, PQQ concentrations over 100 nM were considered to affect
239 plants negatively and were excluded from the follow-up experiments.

240

241 **Transcriptomic landscape of banana plants in response to PQQ**

242 To unveil the molecular roles of PQQ in plants, total RNA was extracted from the CK
243 and 100 nM PQQ treatments, respectively, and used for the following transcriptomic

244 analysis. Totally ~6.5 Gb raw reads were obtained from each sample through the Illumina
245 Hiseq4000 2 x 150 bp sequencing. After mapping the resultants to the banana reference
246 genome (NCBI TaxID: 214687), a total of 25,070 variables were identified (Fig. 4A). Among
247 them, 1,181 and 592 differentially expressed genes (DEGs) were identified through gene
248 ontology (GO) enrichment analysis ($p < 0.05$ and FC >2) and Kyoto Encyclopedia of Genes
249 and Genomes (KEGG) analysis ($p < 0.05$ and FC >1), respectively (Fig. 4B,C).

250 The GO analysis showed that molecular function terms like regulations in heme
251 binding, peroxidase activity, ATPase activity, etc. were found to be enriched regulated.
252 Several DEGs were identified as involved within the chloroplast and mitochondria-related
253 metabolisms within biological processes and cell components terms (Fig. 4B). For KEGG,
254 the DEGs were assigned to 92 pathways, and the 11 pathways, including phenylpropanoid
255 biosynthesis, plant hormone signal transduction, ABC transporters, MAPK signalling
256 pathway – plant, plant-pathogen interaction, etc., were further targeted as they were
257 identified as enriched regulated from both down- and up-regulated (Fig. 4C). The detailed
258 profiles of GO and KEGG analyses were provided in supporting information (Tables S6,S7).
259 Besides, the DEGs were accessed to 11 metabolic pathways or enzymatic genes for further
260 analysis based on our enrichment analysis and previous studies to explore the molecular
261 roles participating within plant physiology (Figs. 4D,S4-S19). Considering the transmission
262 of PQQ across the host and microbe, the ABC transporters ABCB1 and ABCG2/PDR5,
263 which are capable of transporting small molecules, were identified as being regulated with
264 statistical significance (Figs. 4D, S4). Echoing previous works that showed that PQQ has
265 reactive oxygen species (ROS) scavenging and stress-resilience availabilities, 16 and 10
266 genes of glutathione and peroxisome metabolisms were found to be differentially regulated,
267 respectively (Figs. 4D,S5,S6).

268 Interestingly, abundant genes responsible for plant respiration and energic
269 metabolisms were found mainly mediated: genes encode essential proteins for the TCA
270 cycle (*e.g.*, citrate synthase, aconitase, isocitrate dehydrogenase, α-ketoglutarate
271 dehydrogenase and malate dehydrogenase) (Figs. 4D,S7) and oxidative phosphorylation
272 (*e.g.*, plasma membrane ATPase, V-type proton ATPase, mitochondrial external alternative
273 NAD(P)H-ubiquinone oxidoreductase B2 and cytochrome c) (Figs. 4D,S8). Genes involved
274 in the glycolysis/gluconeogenesis pathway and pyruvate metabolism (*e.g.*, acetyl-CoA
275 synthetase, aldo-keto reductase, dihydrolipoyl dehydrogenase, phosphoenolpyruvate
276 carboxylase, pyruvate kinase, pyruvate phosphate dikinase, etc.) were also been up-
277 regulated (Fig. 4D,S9,S10) (Table S7). These results strengthen the perspectives on the
278 participation of PQQ in intercellular electron transmission and redox reactions in plant cells.
279 We also analysed those enriched regulated NAD/NADP-dependent enzymes and
280 dehydrogenase to dig into their coordination (Table S8). Although PQQ was mostly
281 suggested to mediate lactate dehydrogenases in animal and microbial cells, these
282 regulations were not found significantly within plant cells. Instead, its regulations on the
283 other dehydrogenases corresponding to aldehyde, malate, glutamate, isocitrates, etc., while
284 ferredoxin reductases were identified as enrichment with significance (Fig. 4D) (Table S7).

285 This result distinguishes the divergence of molecular roles and functions of PQQ as
286 (NAD/NADP-dependent) dehydrogenase among different life kingdoms.

287 In view of the PGP and anti-*Fusarium* properties of PQQ, the DEGs involved in
288 phenylpropanoid metabolisms, phytohormone biosynthesis and signal transduction, the
289 MAPK signalling pathway, and plant-pathogen interaction were focused. Among them, the
290 phenylpropanoid metabolism for the biosynthesis of structural lignin components, which
291 were essential to the plant cell wall construction and strength and rigidity, were been
292 induced (Fig. S11). The tryptophan metabolism for indole acetate (IAA) and biosynthesis
293 pathways of several chemicals with biotic or abiotic stresses alleviating and with antioxidant
294 activities like lutein and zeaxanthin, carotenoids, dopamine, melatonin and flavonoids were
295 also found induced by PQQ (Fig. S12-S16). For plant hormone signal transduction
296 regulations, auxin and stress-associated pathways were particularly regulated, and
297 pathways for those stress hormones, e.g., ethylene, jasmonic acid, and salicylic acid, were
298 significantly enhanced (Fig. S17). Furthermore, in a total of 23 DEGs of the plant's MAPK
299 signalling and plant-pathogen interaction, metabolisms were also induced, which included
300 various pathogen-associated transcriptional factors, ethylene regulations and pathogenesis-
301 related proteins, suggesting putative immune responses to protecting plants against
302 pathogens could be pre-triggered by the exogenous supplementation of PQQ (Figs.
303 S18,S19).

304

305 **Exogenous supplementation of PQQ boosts the immunity of banana plants**

306 The transcriptomics results confirmed previous findings that mutagenesis of PQQ
307 biosynthesis genes negatively impacts microbial biocontrol ability in plants (20, 21, 39).
308 These results also supported our hypothesis that PQQ coordinates plant growth and
309 immunity to protect the host plant against pathogens. To determine if the antifungal activity
310 observed in tissue culture (Figs. 4A, 5A) persists under soil growing conditions, we
311 transplanted banana plants treated with different concentrations of PQQ into soil pots
312 infected with Foc TR4. We then evaluated four indicators of Panama Disease—leaf
313 yellowing (LY), pseudostem splitting (SS), pseudostem bending (SB), and rhizome dark
314 brown discolouration (RB)—to assess the role of PQQ in protecting plants against *Fusarium*
315 wilt of bananas (Fig. 5B, C). Three months after the *Foc* TR4 infection, the Panama Disease
316 indicators of plants growing in soil conditions were investigated. The unweighted pair group
317 method with arithmetic mean (UPGMA) dendrogram clustering and the principal component
318 analysis (PCA) were performed for an integrative evaluation of the diseasing patterns. The
319 UPGMA results indicated that the LY, RB, and SB diseasing patterns of all PQQ treatments
320 were much closer to the negative control (health plants) than the positive control (diseased
321 plants) (Fig. 5D-F). Alike clustering results were found in P50, P100, and P1000 for the SS
322 diseasing patterns, except for P05 (Fig. 5G).

323 A follow-up PCA suggested a similar result to the UPGMA that the PQQ treatments,
324 especially P50 and P100, help to protect bananas against *Foc* TR4 to stand healthier like
325 those non-infected plants ((Fig. 5H-J). Notably, in addition to those DEGs well-known in
326 phytoalexin accumulation and the plant's systemic immunity induction (Fig. 4D), genes
327 encoding pathogenesis-related protein 1, chitinase, polyphenol oxidase, putative
328 glucuronosyltransferase PGSIP8, 3-ketoacyl-CoA synthase, WRKY transcription factor and
329 disease resistance protein RGA2, were found to be highly regulated (Fig. 5K) (Table S8).
330 These genes have been reported to be highly expressed and critical in the immunity of wild
331 bananas against *Fusarium* wilt (40). Collectively, exogenous supplementation of 100 nM
332 PQQ in the early growing stage not only promotes the organ development of banana
333 plantlets but also triggers the plant's systemic immunity, protecting bananas against
334 *Fusarium* wilt either in tissue culture or in soil. These results suggested that the exogenous
335 supplementation of PQQ to bananas in their early growth stage could contribute to
336 triggering plant immune systems similar to wild bananas to combat *Fusarium* wilt, providing
337 an untapped opportunity for in-field disease maintenance of the banana industry.

338

339 ## Discussion

340 ### Molecular roles of endophytic PQQ in plant-microbe mutualisms

341 On account of being a redox cofactor to types of dehydrogenases, PQQ participates
342 in multiple essential metabolisms across kingdoms. Several studies have reported its effects
343 on either prokaryotic or eukaryotic systems: acting as a strong antioxidant to scavenge
344 reactive oxygen species (41), regulating the balance of nicotinamide adenine dinucleotide
345 (9), inducing mitochondrial biogenesis (10, 11), driving the oxidative phosphorylation and
346 ATP synthesis (12, 13), etc. However, unlike microbes and animals, its molecular roles *in*
347 *planta* remains limited.

348 PQQ has been found to be produced by microbes, prevalent by Gram-negative
349 bacteria (42), and benefits the growth of some plants in different stages (16, 17, 43). In this
350 study, the PQQ exogenous supplementation on bananas and the follow-up transcriptomics
351 (Figs. 3,4) provided new materials and insights into its molecular effects in plants. Our
352 findings suggested that PQQ could affect mitochondrial and energetic metabolisms to
353 improve the overall growth of bananas (Figs. S7-S10), which echoed previous works on
354 animal cells. In addition, multiple phytohormone signalling pathways and photosynthesis of
355 banana plants were also found to be coordinated (Figs. 4,S17). These results provided
356 clues about the molecular roles of PQQ in plants and revealed the molecular roles of
357 endophytic PQQ in mutualistic relationships between plants and microbes.

358 On the other hand, research showed that the disruption of *pqq* genes causes the loss
359 of microbial antifungal activities (20, 21). Han et al. also determined the expression change
360 of a few genes participating in plant immunity, proposing the putative involvement of PQQ in
361 molecular plant-microbe-pathogen tripartite interactions (20). Herein, we confirmed that
362 PQQ has no anti-fungal activity *in vitro* (Fig. 2C) but induces plant immunity *in planta* to
363 protect banana plants against *Fusarium* wilt (Figs. 4-6,S17-S19). Interestingly, the seven
364 immune-related genes with continuously high expression levels of a commercial *Fusarium*-
365 resilient banana cultivar (40) were also found to be highly expressed within banana plants
366 after being treated with 100 nM PQQ (Fig. 5K) (Table S8). This result highlights the potential
367 of endophytic biostimulants, as PQQ here, in breeding biofortification or resistance that
368 achieves similar aims but via fewer costs, deserving more attention for future agriculture.

369

370 ### Evolutionary and functional divergence of PQQ

371 Although the chemical mechanisms of PQQ biosynthesis have been well studied
372 (44), the biosynthesis origin and evolution of this highly conserved order of open reading
373 frame within the *pqq* operon remain unclear. Shen et al. determined the distribution of the
374 main components*, i.e., pqqABCDE*, of the *pqq* operon over 126 prokaryotes (42). Similarly,
375 the *pqq* operon was identified from nearly all genomes of *Burkholderia* species, including

376 environmental isolates, pathogens and symbionts (Fig. 1). In this work, further comparative
377 genomics targeting the *pqq* operon was performed with the purpose of promoting our
378 understanding of such unclear evolutionary linkages between the species.

379 Interestingly, the result showed an environmental isolate *B. cenocepacia* BCMSMB
380 has two copies of the *pqq* operon (*pqqABCDE*, WL90_31170-31190 and *pqqBCDE*,
381 WL90_32390-32405) (Figs. 1B,S20). The incomplete operon was phylogenetically close to
382 *B. cenocepacia*, while the complete one was distinct to both species. Moreover, the
383 complete operon was further found to be located at a predicted gene island (Fig. S20B),
384 suggesting an occurrence of potential evolution events like inter-species horizontal gene
385 transfer. Besides, the *pqq* operon of a *B. seminalis* sub-group (BS0018+BS1628 clade)
386 seemed to get lost during their evolution. Further checking on the amino acid sequences of
387 the operon, a total of nine single amino acid polymorphisms (SAPs) between the species,
388 five in PqqB, two in PqqC and two in PqqE, were identified by multiple sequence alignment
389 (Fig. S21). The phylogenic trees constructed by amino acid sequences also distinguished
390 two species into different clades (Fig. S22). The catalyst within a PqqA/D/E complex is
391 considered the radical beginning of the PQQ biosynthesis, and the products of spontaneous
392 cyclisation after the PqqB-catalysed reaction is the substrate of PqqC in the final step of
393 PQQ biogenesis (44). Our comparative genomics revealed the potential evolutionary events
394 and phylogenic divergences of the operon, especially PqqB, PqqC and PqqE, of virulence
395 and non-virulence *Burkholderia* strains from different hosts and habitats. The results also
396 shed new light on studying the obscure roles of PQQ among molecular host-microbe
397 interactions and their evolution.

398 Moreover, distinct from participating as a cofactor for lactate dehydrogenase in
399 animal and microbial cells, our transcriptomic result suggested that PQQ mainly involve
400 regulations related to aldehydes and carboxylic acids in plant cells (Fig. 4D) (Table S7).
401 These differences may be due to the metabolic preference of lactate and ethanol
402 metabolisms in plant cells across the evolution and the results of host-symbiotic co-
403 evolution over time. A better understanding of such evolutionary and functional divergence
404 among lives is believed to provide great potential for academia and industry towards
405 sustainable agriculture. Beyond, some intriguing topics remain for future research, e.g., why
406 and how do non-PQQ-producing organisms, especially in eukaryotic cells like plants, utilise
407 PQQ? To better understand these questions, comprehensive investigations using integrated
408 approaches among PQQ participating host-microbe interactions are necessary for follow-up
409 research.

410

411 **Conclusion**

412 Previous studies showed the versatile benefits of endophytes to plants in promoting
413 host health and stress resistance (45–48). This work used multi-omics approaches and

414 imaging mass technologies to reveal a PQQ-involving arm racing among molecular plant-
415 endophyte-pathogen interactions. In summary, we demonstrated that *B. seminalis* 869T2
416 produces multiple biostimulants (*e.g.*, PQQ and cyclopeptides) and phytohormones (e.g.,
417 auxins, cytokinins, gibberellins, etc.) to improve the growth of host plants for symbiotic
418 relationships in general conditions; however, when host plants suffer from pathogens, it also
419 secrets antibiotics (*e.g.*, pyrrolnitrin and the derivates) to fight against the attackers (Fig. 2)
420 (Table S4,S5). Meanwhile, the PQQ induces plant immunity to promote the health and
421 resistance of the host plants, thus establishing an endophytic niche in defending those
422 pathogenic invaders (Fig. 6).

423 In conclusion, this is the first work through the omics landscape to explain how PQQ
424 involved plant-endophyte interactions and contributed to plant immunity. These results
425 facilitate our understanding of the realm and highlight PQQ as a potent biostimulant
426 candidate for future agriculture. Beyond the findings presented here, many intriguing
427 questions remain about PQQ in molecular plant-microbe interactions. Why and how do non-
428 PQQ-producing organisms utilize PQQ, particularly in plant cells and the organelles?
429 Further studies on their evolutionary and functional biology are expected to enhance our
430 understanding of this unique microbial redox cofactor in the future.

431

432 ## Materials and methods

433 ### Microbial and plant materials

434 The strain 869T2, *Fusarium oxysporum* f. sp. *cubense* tropical race 4 (*Foc* TR4) and
435 *Arabidopsis thaliana* ecotype Columbia (Col-0) seeds were retrieved from Chieh-Chen
436 Huang Lab's stocks. The plantlets of banana (*Musa acuminata* Cavendish cv. Pei-Chiao)
437 were purchased from Taiwan Banana Research Institute (TBRI), Pingtung, Taiwan.

438 ### Bacterial genome sequencing, assembly and annotation

439 The procedures for genome sequencing and analysis were based on those described
440 in our previous work on bacterial genomes (49–51). The same kits were used following the
441 manufacturer's protocols, and all bioinformatics tools were used with the default settings
442 unless stated otherwise.

443 Briefly, the total DNA of strain 869T2 was extracted and sequenced by Illumina
444 MiSeq 2 × 300 bp paired-end (MS-103-1003) and Oxford Nanopore Technologies (ONT)
445 MinION with R9.4 flow cell (FLO-MIN106) followed by Guppy v3.4.5 for basecalling. A
446 hybrid *de novo* assembly was produced using Unicycler v0.4.9-beta (52). For validation, the
447 Illumina and ONT raw reads were mapped to the assembly using BWA v0.7.12 (53) and
448 Minimap2 v2.15 (54). The results were programmatically checked using SAMtools v1.2 (55)
449 and manually inspected using IGV v2.3.57 (56). For assembly completeness evaluation, the
450 benchmarking universal single-copy orthologous (BUSCO) analysis with the Burkholderiales
451 dataset as a reference was executed on gVolante (57). The finalised assembly was
452 submitted to the National Center for Biotechnology Information (NCBI) and annotated using
453 their Prokaryotic Genome Annotation Pipeline (PGAP) (58). The KofamKOALA (59) was
454 further used to examine putative metabolic pathways.

455 ### Bacterial comparative genomics

456 The genome sequences of *Burkholderia* strains examined by Wallner *et al.* (36),
457 including closely related strains of *B. seminalis* and *B. cenocepacia*, plus an endophyte
458 strain *Paraburkholderia phytofirmans* PsJN (60), were retrieved from NCBI GenBank (61)
459 (accessed on 23 Jul 2021) for comparative analyses with 869T2 (Table S2). FastANI v1.124
460 (62) was used for whole-genome comparison to calculate the proportion of genomic
461 segments mapped and the average nucleotide identity (ANI). The homologous gene
462 clusters were identified using OrthoMCL v1.3 (63) for maximum likelihood phylogeny
463 construction and gene content analysis. These genes were used to produce a concatenated
464 alignment using MUSCLE v3.8.31 (64) for maximum-likelihood inference by PhyML
465 v.3.3.20180214 (65) and visualised using FigTree v1.4.4. PHYLIP v3.69723 (66) was used
466 for bootstrap analysis. For gene content analysis, the previously reported human virulence-
467 facilitating (VIR) and environmental adaptation and MPMI (ENV) related genes were mainly
468 targeted (36). *B. cenocepacia* J2315^{T} and *B. seminalis* LMG24067^{T} were set as the default

469 reference for the VIR and ENV checks, respectively. Given several incomplete genomes
470 were included and the genetic complexity of the *Burkholderia cepacia* complex (BCC),
471 besides homologous gene clusters inferred by OrthoMCL, an additional manual check on
472 the gene length and annotation was also carried out with BLASTP v2.6.0 (67) with e-value
473 cut-off set to 1e-15 and the amino acid sequence identity cut-off set to 80%. Lists of
474 targeted genes for gene content analysis were provided as supporting information (Table
475 S3).

476 **Imaging mass spectrometry analysis**

477 Strain 869T2 was first incubated in LB media at 28°C for 24 hours and then
478 transplanted 2 μL of bacterial culture to a PDA plate as a spot. The spot was incubated
479 alone, or a 4 mm mycelial plug of *Foc* TR4 from a 7-day fungal plate was placed at the
480 opposite edge of the bacterial spot for the dual incubation for five days to monitor the
481 metabolic changes by using matrix-assisted laser desorption/ionisation (MALDI) time-of-
482 flight (TOF) imaging mass spectrometry (IMS). All procedures and settings followed the
483 previously described unless otherwise stated (68, 69). Briefly, the sample areas of agar
484 containing the bacteria alone or with fungal mycelia were excised and transferred onto the
485 MALDI stainless steel target plate. A 1:1 mixture of α-cyano-4-hydroxycinnamic acid and
486 2,5-dihydroxybenzoic acid (universal matrix, Sigma-Aldrich) was spread on top of the
487 samples, then exposed in a 37˚C incubator overnight until it was deemed dried. The IMS
488 data were collected using a Bruker Autoflex Speed MALDI-TOF/TOF mass spectrometer
489 (Bruker Daltonik GmbH, Bremen, Germany) with the following setting: 1000 shots/raster,
490 19.0 and 16.6 kV for the ion sources 1 and 2, 8.7 kV for the lens, 21 and 9.4 kV for
491 reflectors 1 and 2, respectively. The mass ranges from m/z 100-2000 with 25% laser power,
492 positive and reflectron mode was selected, and the raster was set to 800 μm. The universal
493 matrix and peptide standard I (Bruker Daltonik GmbH, Bremen, Germany) were used for MS
494 calibration. All IMS data were processed with TIC normalisation mode and analysed using
495 Fleximaging 3.3 (Bruker Daltonik GmbH, Bremen, Germany).

496 ***In vitro* antagonism assay**

497 The *in vitro* anti-*Fusarium* activity was assessed by comparing fungal hyphal growth
498 rates under the presence and absence of the examined targets. All procedures followed
499 previous work (28) with minor modifications. Strain 869T2 was set as the positive control,
500 and the ddH_2O was used as the mocking negative control. Three concentrations of PQQ
501 (10^2, 10^4 and 10^6 nM) were examined. The antagonistic plate images were photographed,
502 the fungal hyphal growth was measured through ImageJ (70), and the antifungal efficiency
503 (AE) was calculated by AE = (DC-DT)/DC x 100%. DC and DT are *Foc* TR4 colony
504 diameters of the negative control and the comparing target, respectively.

505 **Exogenous supplementation of pyrroloquinoline quinone to plants**

506 The banana plantlets were grown with MS media in the NCHU plant growth chamber
507 as previously described (28) with synthetic PQQ supplementation in different concentrations
508 (Experiment I: 0, 5, 50, 100 and 1000 nM; Experiment II: 0, 100, 1000 and 2000 nM).
509 Phenotypes were photographed, and the growth indicators of visible root formation rate,
510 average leaves number and distribution, plant height, fresh weight, etc., were recorded to
511 determine the plant-growth-promoting (PGP) effects and efficient working dosage of PQQ in
512 plants. Besides, the PQQ-treated banana plantlets were normalised and then transplanted
513 into soil pots, moved to the NCHU greenhouse as described above, and then used for the
514 following *Fusarium* infection assay.

515 ***Fusarium* infection assay and Panama disease resistance evaluation**

516 All procedures of the infection assay carried out in tissue culture containers or soil
517 pots were followed in previous works (28) unless otherwise stated. *Foc* TR4 infectious
518 inocula were prepared in a final concentration of 10^6 conidia per mL. For the tissue culture
519 system, a 5 mm diameter filter paper disc soaked within the infectious inocula was placed at
520 the centre of the banana plantlets for the infection. For the soil pot system, the bananas
521 were domesticated in the NCHU greenhouse and then infected by transplantation into pots
522 containing *Foc* TR4, with a final concentration of 2.8×10^3 spores per gram of soil. The
523 planting matrixes prepared with and without *Foc* TR4 were set as the positive (CKp = CKp2)
524 and negative control (CKn = CKn2), respectively. Four indicators of Panama disease, *i.e.*,
525 leaf yellowing (LY), pseudostem splitting (SS), rhizome (RB) and pseudostem dark brown
526 discolouration (SB) (71), and plant morbidity were determined three months after the
527 infection. Plants without and with LY/SS/SB were recorded as 0 and 1, respectively; plants
528 with RB were recorded as 0, 1, 2 and 3 according to the severity of none, low, medium and
529 high (72); dead plants were weighted by adding 1 to the total score. The fully-scored virtual
530 positive control (CKp1) and zero-scored virtual negative control (CKn1) were also included
531 to assist the follow-up analyses.

532 The principal component analysis (PCA) and the unweighted pair group method with
533 arithmetic mean (UPGMA) were used to analyse the above score data to evaluate the
534 contribution of exogenous supplementation of PQQ to Panama disease resistance. The
535 statistical analyses were performed in R version 4.3.2 (73). For PCA, the function prcomp()
536 was used for primary analysis, and the result was plotted by using the function
537 fviz_pca_biplot(). For UPGMA, the function pvclust() with the distancing method of
538 "Euclidean", hierarchical clustering method of "average", and 1,000 times multiscale
539 bootstrap re-samplings were performed. FigTree v1.4.4 was used for the tree visualisation.
540 To test the effect of the clustering method, we also used the function dist() for calculating
541 the Euclidean distancing-based similarity matrix calculation, then used the function upgma()
542 to construct the dendrogram. As both alternatives produced the same clustering suggestion,
543 only the result based on the pvclust() method with multiscale bootstrap analysis was
544 reported.

545 **Plant total RNA extraction and transcriptomic analysis**

546 The RNA sequencing and analysis procedures were based on those presented in our
547 previous works on plant transcriptomics (50, 72, 74). All kits were used according to the
548 manufacturer's protocols, and all bioinformatics tools were used with the default settings
549 and followed Welgene Biotech's in-house pipeline unless stated otherwise. Banana plantlets
550 were harvested after 11 weeks and grown in ½ MS media with the 100 nM PQQ (treatment)
551 and without PQQ (control), respectively. Total RNA was extracted from the mixtures of three
552 bananas for each treatment using Trizol reagent. The library constructions were generated
553 using TruSeq Stranded mRNA Library Prep Kit (RS-122-2101; Illumina, San Diego, CA
554 USA) and assessed to Agilent Bioanalyzer 2100 system using DNA High Sensitivity Chips
555 for qualification. Illumina Hiseq 4000 platform was used for 150-bp paired-end sequencing.
556 Illumina's program bcl2fastq v2.20 was used for basecalling, and Trimmomatic v0.3642 (75)
557 was implemented to trim off low-quality reads based on Q20 accuracy. The resultant was
558 mapped to *Musa acuminata* subsp. *malaccensis* (NCBI: txid214687) genome (76) using
559 HISAT2 (77). The transcript per million (TPM) method was used for normalisation; genes
560 with low expression levels (< 0.3 TPM value) were excluded. Genes with at least 2.0-fold
561 differences and a probability of at least 0.95 were defined as differentially expressed genes
562 (DEGs). StringTie v2.1.4 (78) and DEseq2 v1.28.1 (79) were used for genome bias
563 detection/correction. Gene set enrichment analysis (GSEA) (80), Gene Ontology (GO) (81)
564 and Kyoto Encyclopedia of Genes and Genomes (KEGG) databases (82) were accessed
565 for the metabolic analyses.

566 **Statistics**

567 The Shapiro-Wilk test and Levene's test were used to check the normal distribution
568 of variables and homoscedasticity, respectively. One-way ANOVA analysis with Tukey's
569 post hoc HSD test for parametric analysis or Kruskal-Wallis test with Dunn's post hoc test
570 for non-parametric analysis was performed to estimate the statistical significance between
571 samples. The data analysis was performed using the Real Statistics Resource Pack v7.7.1
572 (83). At least three independent biological replicates were tested for all experiments, and
573 data are mainly shown as mean ± SE. *$P \leq 0.05$, **$P \leq 0.01$, ***$P \leq 0.005$ and ****$P \leq 0.001$
574 indicated significant differences between samples; otherwise, no significance.

575

Acknowledgements

The Illumina MiSeq and ONT MinION sequencing services for bacterial genome was provided by the Genomic Technology Core (Institute of Plant and Microbial Biology, Academia Sinica). The RNA-seq services were provided by Welgene Biotech Co., Ltd. (Taipei, Taiwan) and Genomics BioSci & Tech Co., Ltd. (Taipei, Taiwan). We thank the technical assistance and the support from Taiwan Banana Research Institute (TBRI), Pingtung, Taiwan and Taichung District Agricultural Research and Extension Station, Ministry of Agriculture of Taiwan.

Author Contributions

SHWH, MYY and CCH designed research; CCH and CHK acquired funding; CCH supervised the project; SHWH, MYY, CHL, TCH, JHP, YLY and YNH performed research; SHWH, CHL, TCH, JHP and YNH analysed data; SHWH wrote the paper - original draft; SHWH, JHP, NYJ, CHK, YNH, EPIC, HHH and CCH wrote the paper - review & editing.

Funding

This work was supported by the National Science and Technology Council of Taiwan (MOST 107-2321-B-005-009; MOST 108-2321-B-005-004; MOST 109-2321-B-005-025; MOST 110-2321-B-005-008), the Ministry of Agriculture of Taiwan (110AS-1.6.1-BQ-B3), and the Ministry of Education of Taiwan (the Higher Education Sprout Project) to Chieh-Chen Huang and Academia Sinica to Chih-Horng Kuo. The funders had no role in study design, data collection and interpretation, or the decision to submit the work for publication.

Data availability

The complete genome sequence of *Burkholderia seminalis* 869T2 has been deposited in GenBank under the accession numbers CP072520-22. The bacterial genome and the plant transcriptome sequencing project, including the associated raw reads, have been deposited in the NCBI under BioProject PRJNA243842 and BioProject PRJNA786465, respectively.

602 ## References

603 1. J. G. Hauge, Kinetics and specificity of glucose dehydrogenase from Bacterium
604 anitratum. *Biochimica et Biophysica Acta* **45**, 263–269 (1960).

605 2. S. A. Salisbury, H. S. Forrest, W. B. T. Cruse, O. Kennard, A novel coenzyme from
606 bacterial primary alcohol dehydrogenases. *Nature* **280**, 843–844 (1979).

607 3. L. Chistoserdova, S.-W. Chen, A. Lapidus, M. E. Lidstrom, Methylotrophy in
608 Methylobacterium extorquens AM1 from a genomic point of view. *J Bacteriol* **185**,
609 2980–2987 (2003).

610 4. J. A. Duine, The PQQ story. *J Biosci Bioeng* **88**, 231–236 (1999).

611 5. M. Matsutani, T. Yakushi, Pyrroloquinoline quinone-dependent dehydrogenases of
612 acetic acid bacteria. *Appl Microbiol Biotechnol* **102**, 9531–9540 (2018).

613 6. M. Naveed, K. Tariq, H. Sadia, H. Ahmad, A. S. Mumtaz, The life history of
614 pyrroloquinoline quinone (pqq): a versatile molecule with novel impacts on living
615 systems. *IJMBOA* **1**, 29–46 (2016).

616 7. C. Anthony, Pyrroloquinoline quinone (PQQ) and quinoprotein enzymes. *Antioxid*
617 *Redox Signal* **3**, 757–774 (2001).

618 8. P. M. Goodwin, C. Anthony, The biochemistry, physiology and genetics of PQQ and
619 PQQ-containing enzymes. *Adv Microb Physiol* **40**, 1–80 (1998).

620 9. K. R. Jonscher, W. Chowanadisai, R. B. Rucker, Pyrroloquinoline-quinone is more than
621 an antioxidant: a vitamin-like accessory factor important in health and disease
622 prevention. *Biomolecules* **11**, 1441 (2021).

623 10. W. Chowanadisai, *et al.*, Pyrroloquinoline Quinone Stimulates Mitochondrial Biogenesis
624 through cAMP Response Element-binding Protein Phosphorylation and Increased
625 PGC-1α Expression*. *Journal of Biological Chemistry* **285**, 142–152 (2010).

626 11. K. Saihara, R. Kamikubo, K. Ikemoto, K. Uchida, M. Akagawa, Pyrroloquinoline
627 Quinone, a Redox-Active o-Quinone, Stimulates Mitochondrial Biogenesis by Activating
628 the SIRT1/PGC-1α Signaling Pathway. *Biochemistry* **56**, 6615–6625 (2017).

629 12. A. Canovai, *et al.*, Pyrroloquinoline quinone drives ATP synthesis in vitro and in vivo
630 and provides retinal ganglion cell neuroprotection. *Acta Neuropathologica*
631 *Communications* **11**, 146 (2023).

632 13. M. C. Ebeling, *et al.*, Improving retinal mitochondrial function as a treatment for age-
633 related macular degeneration. *Redox Biology* **34**, 101552 (2020).

634 14. R. Carreño-López, J. M. Alatorre-Cruz, V. Marín-Cevada, “Pyrroloquinoline quinone
635 (PQQ): role in plant-microbe interactions” in *Secondary Metabolites of Plant Growth*
636 *Promoting Rhizomicroorganisms: Discovery and Applications*, H. B. Singh, C. Keswani,
637 M. S. Reddy, E. Sansinenea, C. García-Estrada, Eds. (Springer, 2019), pp. 169–184.

638 15. M. Ben Farhat, A. Fourati, H. Chouayekh, Coexpression of the pyrroloquinoline
639 quinone and glucose dehydrogenase genes from Serratia marcescens CTM 50650
640 conferred high mineral phosphate-solubilizing ability to Escherichia coli. *Appl Biochem*
641 *Biotechnol* **170**, 1738–1750 (2013).

642 16. Y.-S. Cho, *et al.*, PQQ-dependent organic acid production and effect on common bean
643 growth by Rhizobium tropici CIAT 899. *Journal of Microbiology and Biotechnology* **13**,
644 955–959 (2003).

645 17. O. Choi, *et al.*, Pyrroloquinoline quinone is a plant growth promotion factor produced by
646 Pseudomonas fluorescens B16. *Plant Physiol* **146**, 657–668 (2008).

647 18. L. Li, Z. Jiao, L. Hale, W. Wu, Y. Guo, Disruption of gene pqqA or pqqB reduces plant
648 growth promotion activity and biocontrol of crown gall disease by Rahnella aquatilis
649 HX2. *PLoS One* **9**, e115010 (2014).

650 19. A. H. Patel, V. Chovatia, S. Shah, Expression of pyrroloquinoline quinone in Rhizobium
651 leguminosarum for phosphate solubilization. *Environment and Ecology* **33**, 621–624
652 (2015).

653 20. S. H. Han, *et al.*, Inactivation of pqq genes of Enterobacter intermedium 60-2G reduces
654 antifungal activity and induction of systemic resistance. *FEMS Microbiol Lett* **282**, 140–
655 146 (2008).

656 21. J. Xu, *et al.*, The pqqC gene is essential for antifungal activity of Pseudomonas
657 kilonensis JX22 against Fusarium oxysporum f. sp. lycopersici. *FEMS Microbiology*
658 *Letters* **353**, 98–105 (2014).

659 22. F. Garcia-Bastidas, Fusarium oxysporum f.sp. cubense tropical race 4 (Foc TR4). *CABI*
660 *Compendium* **CABI Compendium**, 59074053 (2022).

661 23. R. C. Ploetz, Fusarium Wilt of Banana. *Phytopathology®* **105**, 1512–1521 (2015).

662 24. TR4 Global Network, TR4 Basics. Available at https://www.fao.org/tr4gn/tr4-basics/en/.
663 Deposited 15 January 2024.

664 25. A. A. Ismaila, *et al.*, Fusarium wilt of banana: Current update and sustainable disease
665 control using classical and essential oils approaches. *Horticultural Plant Journal* **9**, 1–
666 28 (2023).

667 26. G. Bubici, M. Kaushal, M. I. Prigigallo, C. Gómez-Lama Cabanás, J. Mercado-Blanco,
668 Biological Control Agents Against Fusarium Wilt of Banana. *Frontiers in Microbiology*
669 **10**, 616 (2019).

670 27. C. Du, *et al.*, Construction of a compound microbial agent for biocontrol against
671 Fusarium wilt of banana. *Frontiers in Microbiology* **13**, 1066807 (2022).

672 28. Y.-N. Ho, *et al.*, In planta biocontrol of soilborne Fusarium wilt of banana through a
673 plant endophytic bacterium, Burkholderia cenocepacia 869T2. *Plant Soil* **387**, 295–306
674 (2015).

675 29. Z. Zhu, *et al.*, Spatiotemporal biocontrol and rhizosphere microbiome analysis of
676 Fusarium wilt of banana. *Commun Biol* **6**, 1–10 (2023).

677 30. T. Damodaran, *et al.*, Secondary metabolite induced tolerance to Fusarium oxysporum
678 f.sp. cubense TR4 in banana cv. Grand Naine through in vitro bio-immunization: a
679 prospective research translation from induction to field tolerance. *Frontiers in*
680 *Microbiology* **14**, 1233469 (2023).

681 31. L. Zhang, *et al.*, Biocontrol Potential of Endophytic Streptomyces malaysiensis 8ZJF-21
682 From Medicinal Plant Against Banana Fusarium Wilt Caused by Fusarium oxysporum f.
683 sp. cubense Tropical Race 4. *Frontiers in Plant Science* **13**, 874819 (2022).

684 32. Y.-N. Ho, C.-C. Huang, Draft genome sequence of Burkholderia cenocepacia strain
685 869T2, a plant-beneficial endophytic bacterium. *Genome Announcements* **3**, e01327-
686 15 (2015).

687 33. H.-H. Hwang, *et al.*, A plant endophytic bacterium, Burkholderia seminalis strain 869T2,
688 promotes plant growth in Arabidopsis, Pak Choi, Chinese amaranth, lettuces, and other
689 vegetables. *Microorganisms* **9**, 1703 (2021).

690 34. S.-H. W. Hung, *et al.*, Endophytic biostimulants for smart agriculture: Burkholderia
691 seminalis 869T2 benefits heading leafy vegetables in-field management in Taiwan.
692 *Agronomy* **13**, 967 (2023).

693 35. B.-A. T. Nguyen, *et al.*, Biodegradation of dioxins by Burkholderia cenocepacia strain
694 869T2: role of 2-haloacid dehalogenase. *Journal of Hazardous Materials* **401**, 123347
695 (2021).

696 36. A. Wallner, E. King, E. L. M. Ngonkeu, L. Moulin, G. Béna, Genomic analyses of
697 Burkholderia cenocepacia reveal multiple species with differential host-adaptation to
698 plants and humans. *BMC Genomics* **20**, 803 (2019).

699 37. A. Baldwin, P. A. Sokol, J. Parkhill, E. Mahenthiralingam, The Burkholderia cepacia
700 epidemic strain marker is part of a novel genomic island encoding both virulence and

701 metabolism-associated genes in Burkholderia cenocepacia. *Infect Immun* **72**, 1537–
702 1547 (2004).

703 38. S. Pawar, A. Chaudhari, R. Prabha, R. Shukla, D. P. Singh, Microbial Pyrrolnitrin:
704 Natural Metabolite with Immense Practical Utility. *Biomolecules* **9**, 443 (2019).

705 39. Y. B. Guo, *et al.*, Mutations That Disrupt Either the pqq or the gdh Gene of Rahnella
706 aquatilis Abolish the Production of an Antibacterial Substance and Result in Reduced
707 Biological Control of Grapevine Crown Gall. *Applied and Environmental Microbiology*
708 **75**, 6792–6803 (2009).

709 40. L. Zhang, *et al.*, Transcriptomic analysis of resistant and susceptible banana corms in
710 response to infection by Fusarium oxysporum f. sp. cubense tropical race 4. *Sci Rep* **9**,
711 8199 (2019).

712 41. H. S. Misra, *et al.*, Pyrroloquinoline-quinone: a reactive oxygen species scavenger in
713 bacteria. *FEBS Letters* **578**, 26–30 (2004).

714 42. Y.-Q. Shen, *et al.*, Distribution and properties of the genes encoding the biosynthesis of
715 the bacterial cofactor, pyrroloquinoline quinone. *Biochemistry* **51**, 2265–2275 (2012).

716 43. L. B. Xiong, J. Sekiya, N. Shimose, Occurrence of Pyrroloquinoline Quinone (PQQ) in
717 Pistils and Pollen Grains of Higher Plants. *Agricultural and Biological Chemistry* **54**,
718 249–250 (1990).

719 44. Zhu, J. P. Klinman, Biogenesis of the peptide-derived redox cofactor pyrroloquinoline
720 quinone. *Current Opinion in Chemical Biology* **59**, 93–103 (2020).

721 45. S. Card, L. Johnson, S. Teasdale, J. Caradus, Deciphering endophyte behaviour: the
722 link between endophyte biology and efficacious biological control agents. *FEMS*
723 *Microbiol Ecol* **92**, fiw114 (2016).

724 46. P. Chaudhary, U. Agri, A. Chaudhary, A. Kumar, G. Kumar, Endophytes and their
725 potential in biotic stress management and crop production. *Frontiers in Microbiology*
726 **13**, 933017 (2022).

727 47. J. Hallmann, A. Quadt-Hallmann, W. F. Mahaffee, J. W. Kloepper, Bacterial
728 endophytes in agricultural crops. *Can. J. Microbiol.* **43**, 895–914 (1997).

729 48. P. R. Hardoim, *et al.*, The hidden world within plants: ecological and evolutionary
730 considerations for defining functioning of microbial endophytes. *Microbiol Mol Biol Rev*
731 **79**, 293–320 (2015).

732 49. S.-H. W. Hung, M.-C. Chiu, C.-C. Huang, C.-H. Kuo, Complete genome sequence of
733 Curtobacterium sp. C1, a beneficial endophyte with the potential for in-plant salinity
734 stress alleviation. *MPMI* **35**, 731–735 (2022).

735 50. S.-H. W. Hung, *et al.*, A cyclic dipeptide for salinity stress alleviation and the trophic
736 flexibility of endophyte provide insights into saltmarsh plant–microbe interactions. *ISME*
737 *Communications* **4**, ycae041 (2024).

738 51. S.-H. W. Hung, I.-C. Wu, C.-C. Huang, C.-H. Kuo, Complete genome sequence of
739 Erythrobacteraceae bacterium WH01K, a strain isolated from corals (Acropora sp.) in
740 Taiwan. *Microbiology Resource Announcements* **12**, e00830-23 (2023).

741 52. R. R. Wick, L. M. Judd, C. L. Gorrie, K. E. Holt, Unicycler: resolving bacterial genome
742 assemblies from short and long sequencing reads. *PLoS Comput Biol* **13**, e1005595
743 (2017).

744 53. H. Li, R. Durbin, Fast and accurate short read alignment with Burrows-Wheeler
745 transform. *Bioinformatics* **25**, 1754–1760 (2009).

746 54. H. Li, Minimap2: pairwise alignment for nucleotide sequences. *Bioinformatics* **34**,
747 3094–3100 (2018).

748 55. H. Li, *et al.*, The sequence alignment/map format and SAMtools. *Bioinformatics* **25**,
749 2078–2079 (2009).

750 56. J. T. Robinson, *et al.*, Integrative genomics viewer. *Nat Biotechnol* **29**, 24–26 (2011).

751 57. O. Nishimura, Y. Hara, S. Kuraku, Evaluating genome assemblies and gene models
752 using gVolante. *Methods Mol Biol* **1962**, 247–256 (2019).

753 58. T. Tatusova, *et al.*, NCBI prokaryotic genome annotation pipeline. *Nucleic Acids Res*
754 **44**, 6614–6624 (2016).

755 59. T. Aramaki, *et al.*, KofamKOALA: KEGG Ortholog assignment based on profile HMM
756 and adaptive score threshold. *Bioinformatics* **36**, 2251–2252 (2020).

757 60. A. Weilharter, *et al.*, Complete genome sequence of the plant growth-promoting
758 endophyte Burkholderia phytofirmans strain PsJN. *Journal of Bacteriology* **193**, 3383–
759 3384 (2011).

760 61. D. A. Benson, *et al.*, GenBank. *Nucleic Acids Res* **46**, D41–D47 (2018).

761 62. C. Jain, L. M. Rodriguez-R, A. M. Phillippy, K. T. Konstantinidis, S. Aluru, High
762 throughput ANI analysis of 90K prokaryotic genomes reveals clear species boundaries.
763 *Nat Commun* **9**, 5114 (2018).

764 63. L. Li, C. J. Stoeckert, D. S. Roos, OrthoMCL: identification of ortholog groups for
765 eukaryotic genomes. *Genome Res.* **13**, 2178–2189 (2003).

766 64. R. C. Edgar, MUSCLE: multiple sequence alignment with high accuracy and high
767 throughput. *Nucleic Acids Research* **32**, 1792–1797 (2004).

768 65. S. Guindon, O. Gascuel, A simple, fast, and accurate algorithm to estimate large
769 phylogenies by maximum likelihood. *Systematic Biology* **52**, 696–704 (2003).

770 66. J. Felsenstein, PHYLIP - phylogeny inference package (version 3.2). *Cladistics* **5**, 164–
771 166 (1989).

772 67. C. Camacho, *et al.*, BLAST+: architecture and applications. *BMC Bioinformatics* **10**,
773 421 (2009).

774 68. Y.-N. Ho, *et al.*, Specific inactivation of an antifungal bacterial siderophore by a fungal
775 plant pathogen. *ISME J* **15**, 1858–1861 (2021).

776 69. Y.-L. Yang, Y. Xu, P. Straight, P. C. Dorrestein, Translating metabolic exchange with
777 imaging mass spectrometry. *Nat Chem Biol* **5**, 885–887 (2009).

778 70. C. A. Schneider, W. S. Rasband, K. W. Eliceiri, NIH image to ImageJ: 25 years of
779 image analysis. *Nat Methods* **9**, 671–675 (2012).

780 71. Y. Wu, *et al.*, Systemic acquired resistance in Cavendish banana induced by infection
781 with an incompatible strain of Fusarium oxysporum f. sp. cubense. *Journal of Plant*
782 *Physiology* **170**, 1039–1046 (2013).

783 72. M.-Y. Yu, “A study of pyrroloquinoline quinone on Pei-Chiao (Musa spp.) growth and
784 biocontrol improvement,” National Chung Hsing University, Taichung, Taiwan. (2019).

785 73. R Core Team, R: A Language and Environment for Statistical Computing. (2024).
786 Deposited 18 March 2024.

787 74. Y.-H. Tsai, “Transcriptomic analysis on adaptive immunity of Pei-Chiao (Musa spp.,
788 Cavendish AAA) against Fusarium wilt caused by Fusarium oxysporum f. sp. cubense
789 tropical race4.,” National Chung Hsing University, Taichung, Taiwan. (2019).

790 75. A. M. Bolger, M. Lohse, B. Usadel, Trimmomatic: a flexible trimmer for Illumina
791 sequence data. *Bioinformatics* **30**, 2114–2120 (2014).

792 76. A. D’Hont, *et al.*, The banana (Musa acuminata) genome and the evolution of
793 monocotyledonous plants. *Nature* **488**, 213–217 (2012).

794 77. D. Kim, B. Langmead, S. L. Salzberg, HISAT: a fast spliced aligner with low memory
795 requirements. *Nat Methods* **12**, 357–360 (2015).

796 78. M. Pertea, *et al.*, StringTie enables improved reconstruction of a transcriptome from
797 RNA-seq reads. *Nat Biotechnol* **33**, 290–295 (2015).

798 79. M. I. Love, W. Huber, S. Anders, Moderated estimation of fold change and dispersion
799 for RNA-seq data with DESeq2. *Genome Biology* **15**, 550 (2014).

800 80. A. Subramanian, *et al.*, Gene set enrichment analysis: A knowledge-based approach
801 for interpreting genome-wide expression profiles. *Proc. Natl. Acad. Sci. U.S.A.* **102**,
802 15545–15550 (2005).

803 81. H. Mi, A. Muruganujan, D. Ebert, X. Huang, P. D. Thomas, PANTHER version 14: more
804 genomes, a new PANTHER GO-slim and improvements in enrichment analysis tools.
805 *Nucleic Acids Research* **47**, D419–D426 (2019).

806 82. M. Kanehisa, S. Goto, KEGG: Kyoto encyclopedia of genes and genomes. *Nucleic*
807 *Acids Res* **28**, 27–30 (2000).

808 83. C. Zaiontz, Real Statistics Resource Pack software. Available at www.real-
809 statistics.com. Deposited 21 February 2024.

810

811 ## Figure Legends

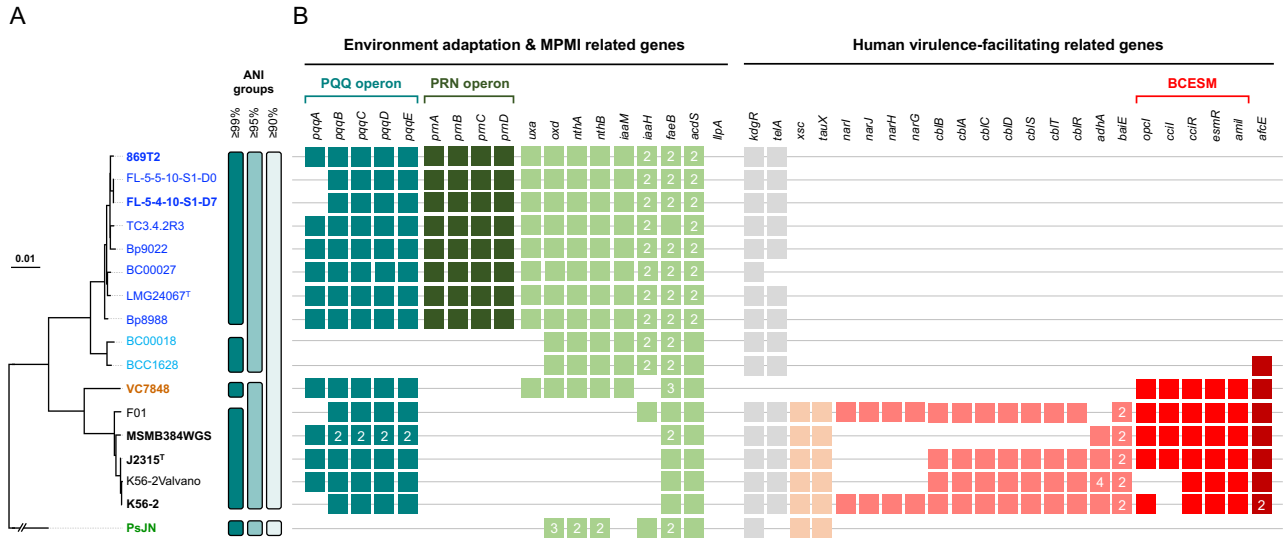

812

813 **Fig. 1 Evolutionary and comparative genomics among strain 869T2 and its relatives. A** Maximum likelihood phylogeny based on a
814 concatenated alignment of 3,018 single-copy genes shared by all genomes (987,390 aligned amino acid sites). All internal nodes received
815 100% bootstrap support based on 1,000 resamplings. *Paraburkholderia phytofirmans* PsJN^{T} is included as the outgroup. The superscripts
816 'T' following the strain names indicate type strains and the complete genomes are presented in bold. Grouping based on different
817 genome-wide average nucleotide identity (ANI) thresholds is plotted to the right of the phylogenic tree. **B** Gene content analysis. The
818 distribution of key genes involved in environmental adaptation, molecular plant-microbe interactions (MPMI), and human virulence-
819 facilitating (VIR) are plotted. The colour boxes indicate gene presence, and the numbers within the boxes indicate copy numbers of multi-
820 copy genes. Abbreviations: PQQ, pyrroloquinoline quinone. PRN, pyrrolnitrin. BCESM, *Burkholderia cepacia* epidemic strain marker.
821 Detailed information regarding the strains and target genes are provided in Table S2 and Table S3, respectively.

822

823

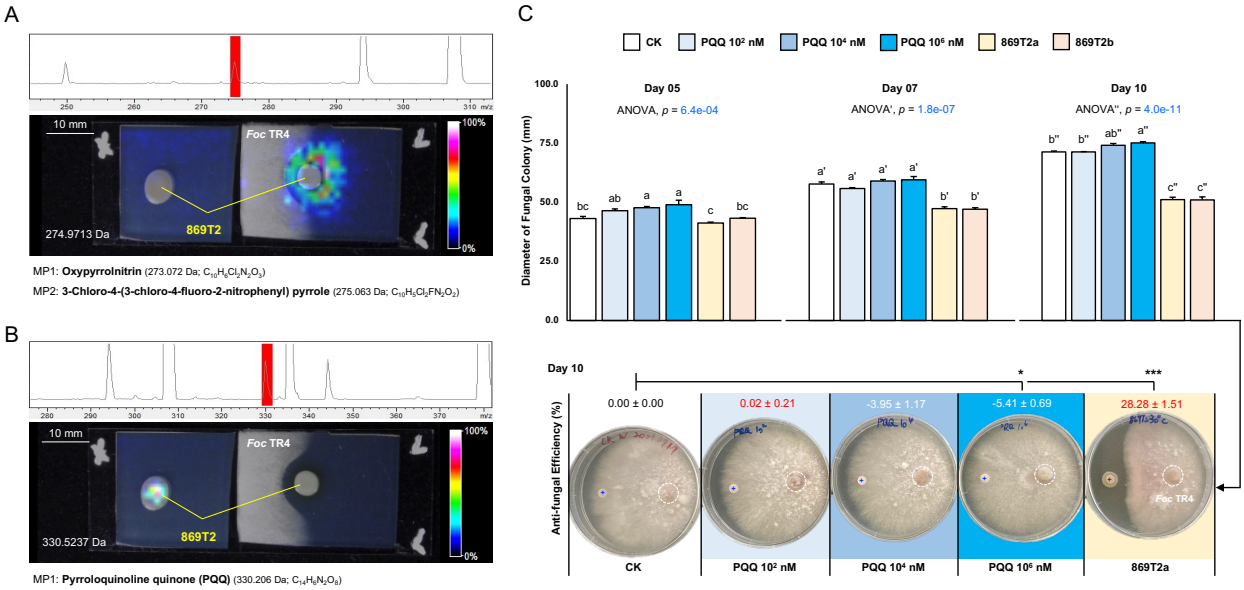

Fig. 2 Identification and quantification of potential endophytic biostimulants. *In situ* imaging mass results of endophyte-pathogen co-incubation under the metabolic signalling detection under **A** 274.9713 m/z and **B** 330.5237 m/z, respectively. 869T2, *Burkholderia seminalis* 869T2. *Foc* TR4, *Fusarium oxysporum* f. sp. cubense tropical race 4. MP, metabolite of prediction. Colour keys refer to the metabolic abundance of detection. **C** Antagonism assay for testing different concentrations of pyrroloquinoline quinone (PQQ) against *Foc* TR4 *in vitro*. PQQ was prepared as 10^2, 10^4, and 10^6 nM for the assay. *Burkholderia seminalis* 869T2 precultured under precultured under 30°C (869T2a) or 37°C (869T2b) was set as the positive control, and the ddH_2O was set as the negative control (CK). The sample disk of each treatment and Foc TR4 were highlighted by a blue cross and a white dashed circle, respectively, within the plate images. Data were presented as mean ± SEM, N = 3. Statistical significances between samples were indicated by different letters ($p<0.05$) or by asterisks (*$p<0.05$; ***$p<0.005$); otherwise, not significant.

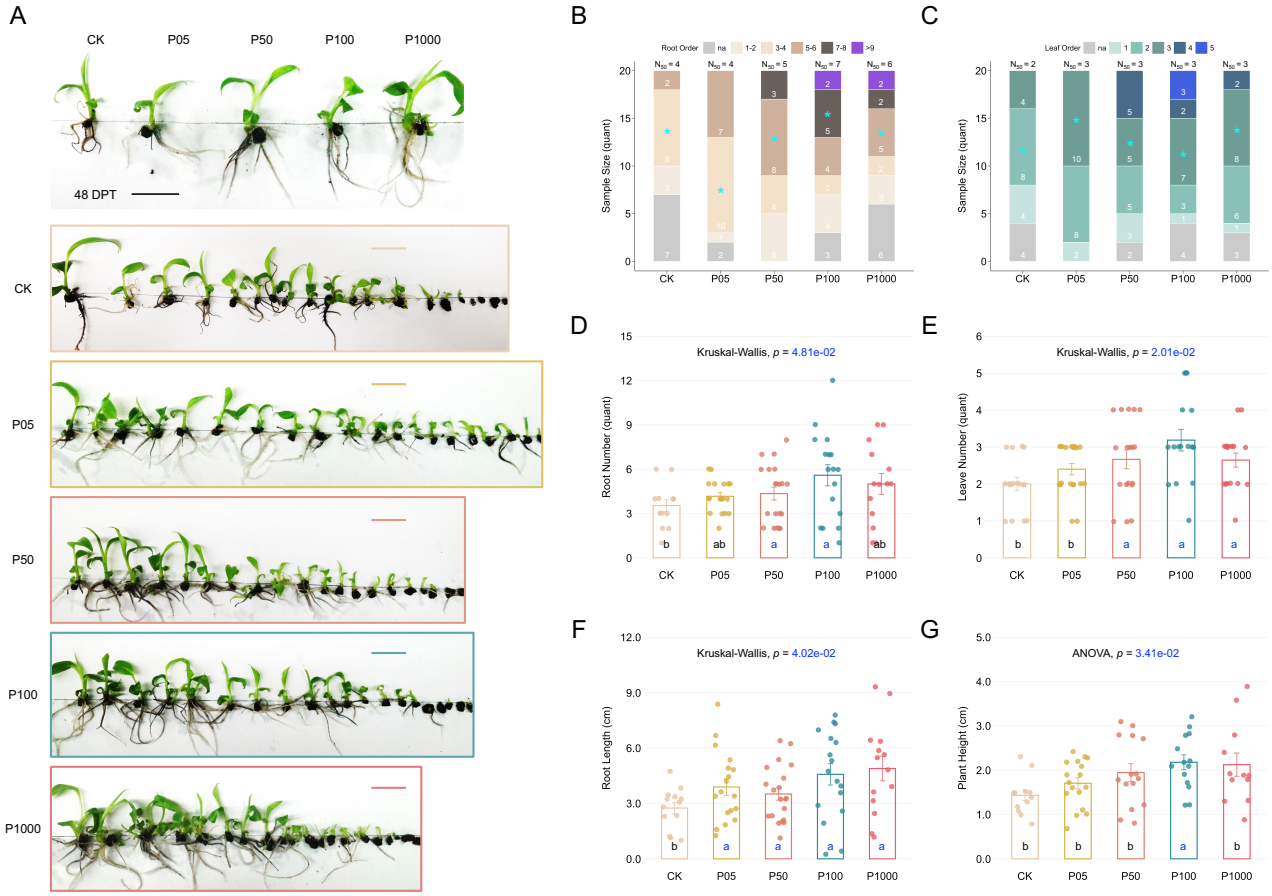

Fig. 3 Exogenous supplementation of PQQ benefits the differentiation and development of banana plants in tissue culture conditions. A Phenotypic photographs of banana plants in response to different concentrations of supplementary pyrroloquinoline quinone (PQQ) at 48 days after treatment (DPT). CK, P05, P50, P100 and P1000 indicate the 0 nM, 5 nM, 50 nM, 100 nM and 1000 nM PQQ treatment, respectively. Scale bars, 3 cm. The distribution of **B** root number and **C** leaf number of banana plants at 48 DPT. Numbers in stacked bar charts indicate the sample size. Asterisks highlight the distribution groups of defined N_{50} for plant growth-promotion evaluation, as mentioned in Materials and Methods. na, non-differentiated samples. **D** Root number, **E** leaf number, **F** root length and **G** plant height of banana plants at 48 DPT, excluding non-differentiated samples in **B** or **C**. Each dot represents a sample. Data are mean ± SEM; different letters indicate significant differences based on multiple comparisons, Tukey method after ANOVA or Dunn method after the Kruskal-Wallis test.

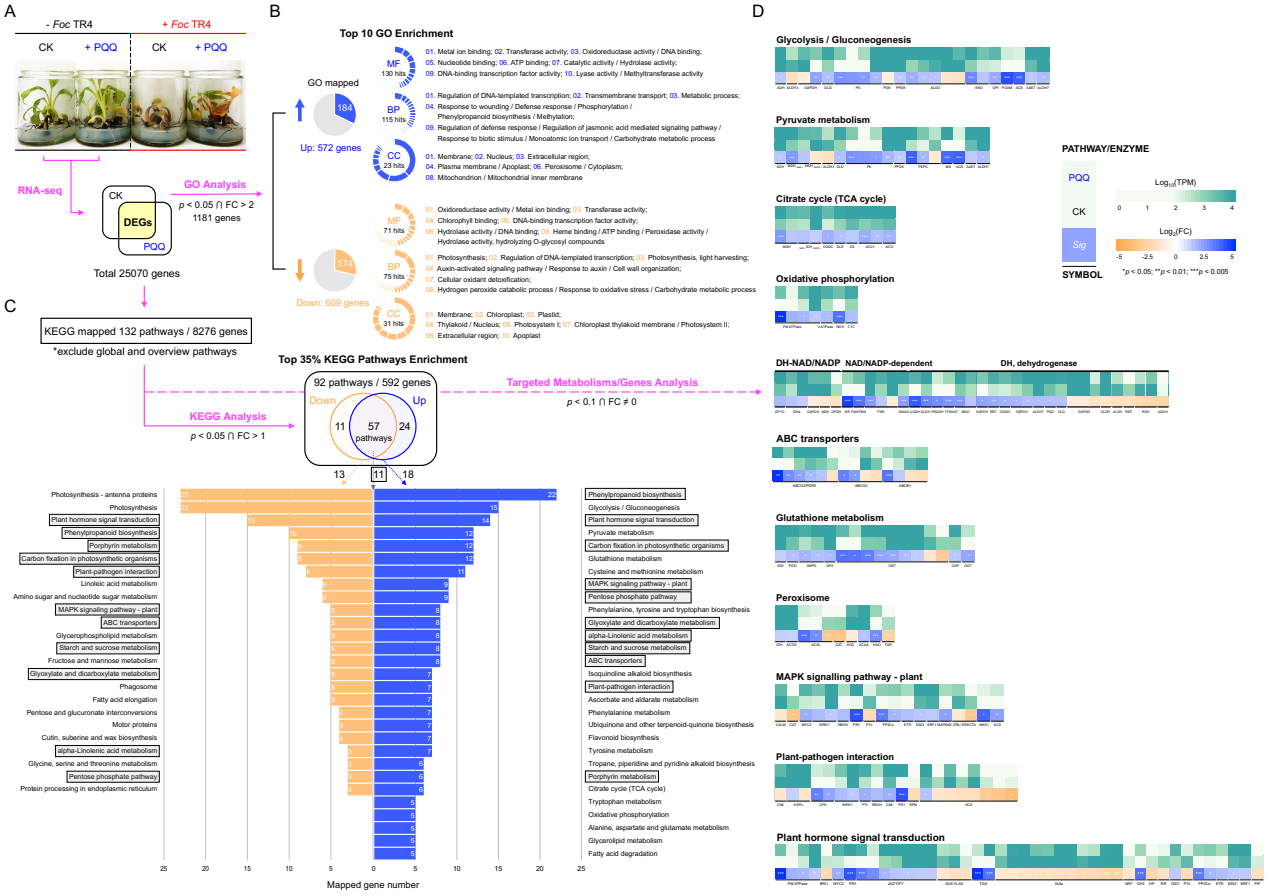

Fig. 4 Transcriptomic landscape of banana plants in response to PQQ. A Phenotypes of banana plant treated with 100 nM PQQ and infected by *Fusarium oxysporum* f. sp. cubense tropical race 4 (Foc TR4) at tissue culture growing stage. Total RNA was collected from these plants for the follow-up transcriptomic analysis. Differentially expressed genes (DEGs) defined by certain criteria were then subjected to **B** Gene Ontology (GO) terms enrichment analysis, **C** Kyoto Encyclopedia of Genes and Genomes (KEGG) pathways analysis and **D** targeted metabolisms and genes expression analysis. **B** The number inside the pie chart indicates the number of mapped GO terms, and the number inside the donut chart indicates the total hits of DEGs by the top 10 mapped GO terms presented orderly at the right of the donut chart. **C** The number inside the pie chart indicates the number of total DEGs-mapped KEGG pathways; the top 35% were labelled beside arrows linking to the column chart below; the number inside the column chart indicates the number of mapped DEGs; those mapped KEGG pathways shared by up- and down-regulated DEGs were marked by grey boxes. **D** Heatmaps showed the specific gene expression of targeted KEGG pathways. Details of gene symbols can be accessed in Table S7. The colour keys refer to the transcripts per kilobase million (TPM) and the corresponding fold changes (FC). Statistical significances between samples were indicated by asterisks (*p<0.05; **p<0.01; ***p<0.005); otherwise, not significant.

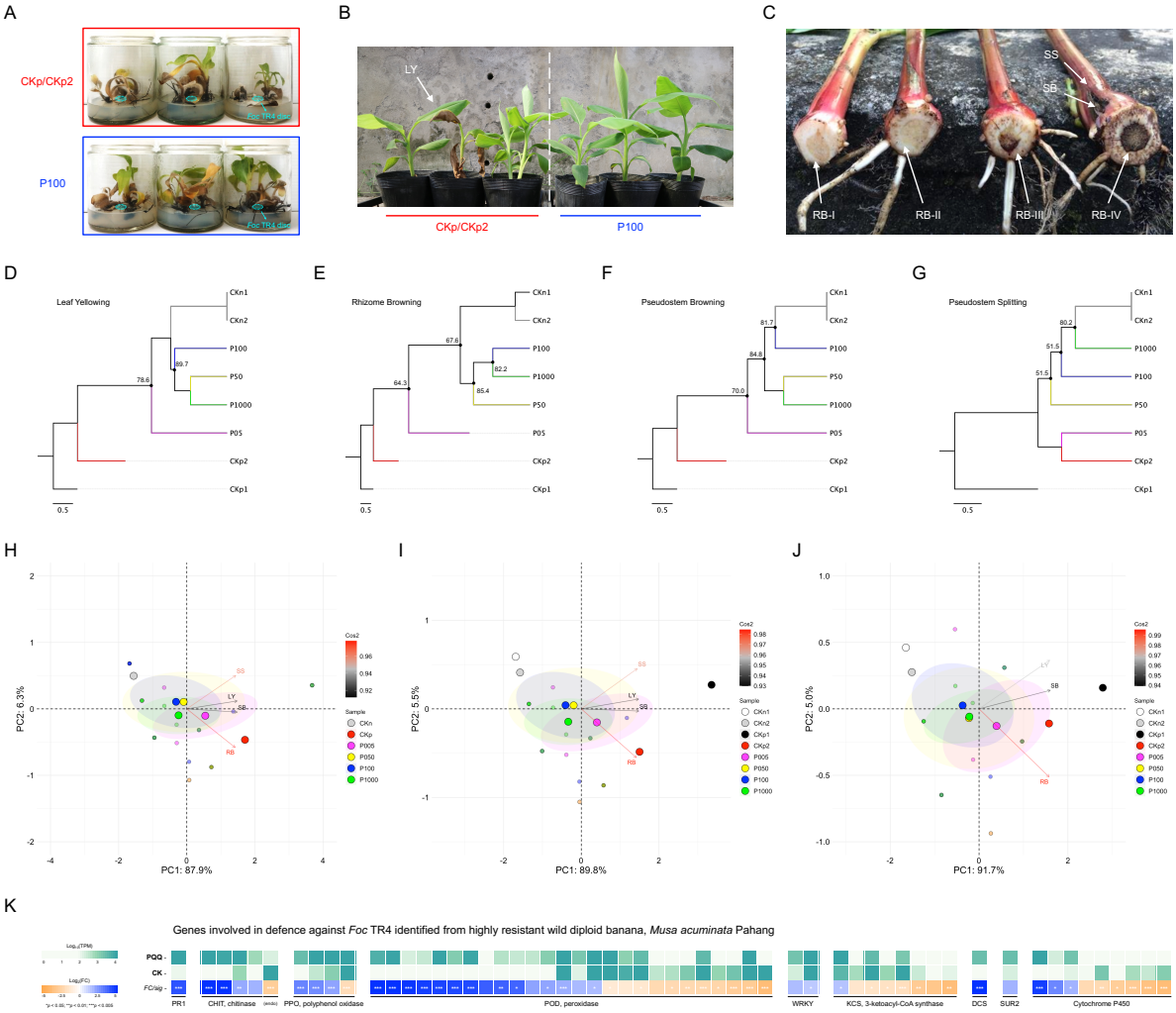

Fig. 5 PQQ contributes to the immunity of banana plants combating *Fusarium* wilt. Exogenous supplementation of PQQ contributes to the tolerance of banana plants against *Fusarium* oxysporum f. sp. cubense tropical race 4 (*Foc* TR4) in **A** tissue culture and in **B** soil conditions. *Foc* TR4 infection was performed through **A** discs (1.0 x 10^6 CFU/mL) placed at the centre of three replicates, highlighted by cyan dashed circles, or through **B** transplantation using infected soil (2.8 x 10^3 spore/gram). CKp/CKp2 and P100 are samples treated by ddH_2O and 100 nM PQQ, respectively. White arrows highlight four phenotypic indicators: **B** leaf yellowing (LY), **C** pseudostem splitting (SS), pseudostem (SB) and rhizome dark brown discolouration (RB) for the Panama disease resistance estimation; roman numerals suffixes of RB indicate the levels of disease severity from low to high as described in Materials and Methods. **D-F** Principal component analysis (PCA) on Panama disease indicators (LY, RB, SB and SS) of non-infected (CKn = CKn2; non-PQQ-pretreated) and Foc TR4-infected banana plants pretreated with different concentrations of PQQ; 0 mM (CKp = CKp2), 5 nM (P05), 50 nM (P50), 100 nM (P100) and 1000 nM (P1000); CKn1 and CKp1 are virtual negative and positive controls, respectively, included to assist the analyses; see Material and Methods for further details. Biplot vectors are the disease indicator loadings, whereas the position of each treatment is shown. Cos2 represents the quality of representation for variables on the factor map. **G-J** Unweighted pair group method with arithmetic mean (UPGMA) clustering dendrograms on Panama disease indicators of banana plants treated with different concentrations of PQQ; the dataset was accessed from **E** The trees were constructed based on the Euclidean distancing method with 1,000 multiscale bootstrap re-samplings; the approximately unbiased p-value of those internal nodes with < 90% were labelled. **K** Heatmaps showed the specific gene expression of genes involved in the immunity of wild bananas combating *Fusarium*. Details of gene symbols can be accessed in Table S8. The colour keys refer to the transcripts per kilobase million (TPM) and the corresponding fold changes (FC). Statistical significances between samples were indicated by asterisks (*p<0.05; **p<0.01; ***p<0.005); otherwise, not significant.

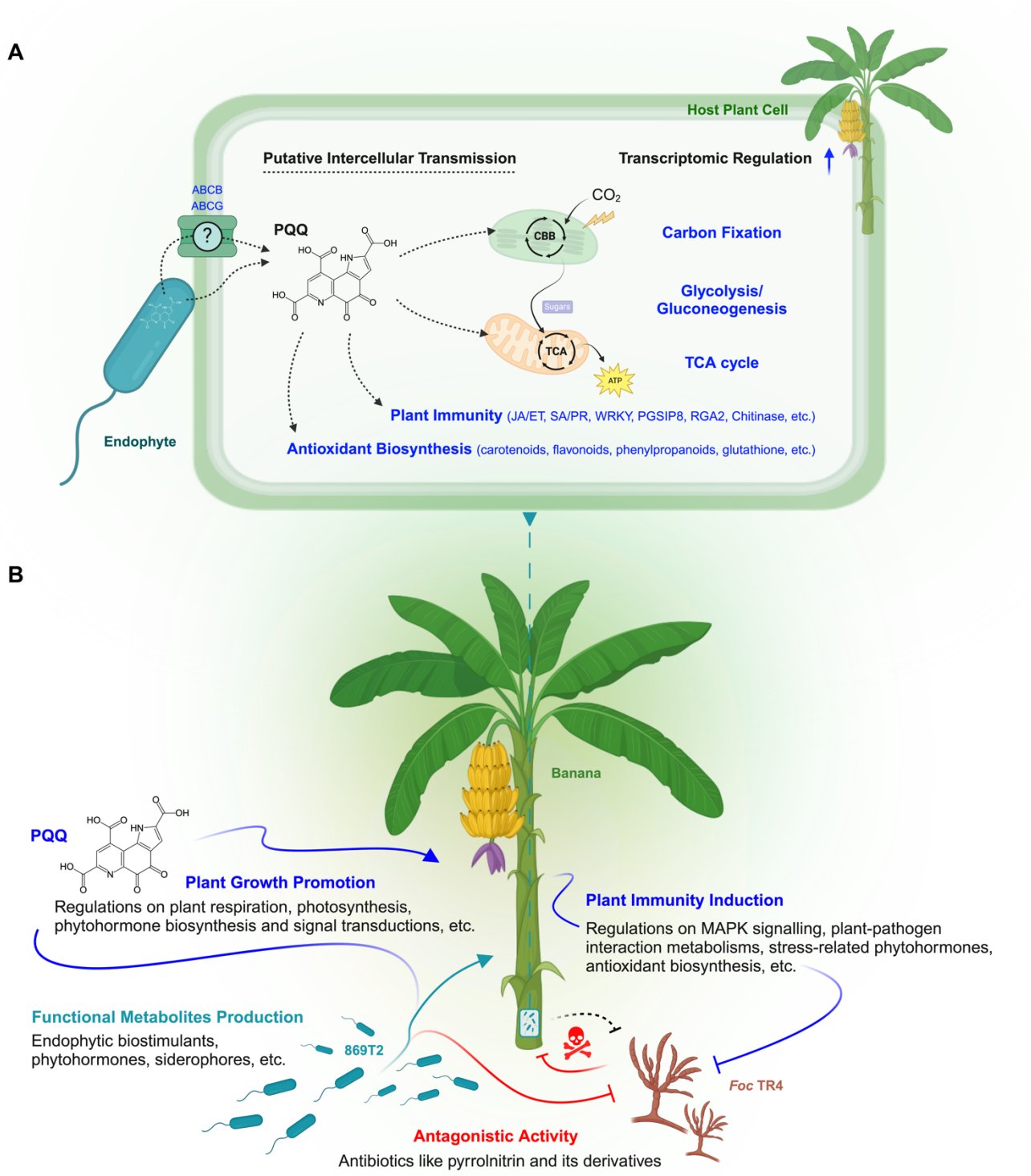

Fig. 6 Schematic illustration of plant-endophyte interactions that PQQ confers endophytic niches by coordinating host development. A Proposed PQQ molecular mechanisms in plant cells. Dashed lines indicate putative transmission from prokaryotic cells to or within eukaryotic cells. The mainly regulated genes and metabolisms identified with transcriptomics were highlighted in blue. **B** An overall viewpoint on how endophytes benefit the health of host plants and combat the *Fusarium* wilt of bananas. Icons were created with BioRender.com.